vol. 159, no. 1 the american naturalist january 2002

Comparing Classical Community Models: Theoretical Consequences for Patterns of Diversity

Jérôme Chave,* Helene C. Muller-Landau,† and Simon A. Levin‡

Department of Ecology and Evolutionary Biology, Princeton University, Princeton, New Jersey 08544-1003

Submitted October 26, 2000; Accepted July 7, 2001

abstract: Mechanisms proposed to explain the maintenance of species diversity within ecological communities of sessile organisms include niche differentiation mediated by competitive trade-offs, frequency dependence resulting from species-specific pests, recruitment limitation due to local dispersal, and a speciation-extinction dynamic equilibrium mediated by stochasticity (drift). While each of these processes, and more, have been shown to act in particular communities, much remains to be learned about their relative importance in shaping community-level patterns. We used a spatially-explicit, individual-based model to assess the effects of each of these processes on species richness, relative abundance, and spatial patterns such as the species-area curve. Our model communities had an order-of-magnitude more individuals than any previous such study, and we also developed a finite-size scaling analysis to infer the large-scale properties of these systems in order to establish the generality of our conclusions across system sizes. As expected, each mechanism can promote diversity. We found some qualitative differences in community patterns across communities in which different combinations of these mechanisms operate. Species-area curves follow a power law with short-range dispersal and a logarithmic law with global dispersal. Relative-abundance distributions are more even for systems with competitive differences and trade-offs than for those in which all species are competitively equivalent, and they are most even when frequency dependence (even if weak) is present. Overall, however, communities in which different processes operated showed surprisingly similar patterns, which suggests that the form of community-level patterns cannot in general be used to distinguish among mechanisms maintaining diversity there. Nevertheless, parameterization of models such as these from field data on the strengths of the different mechanisms could yield insight into their relative roles in diversity maintenance in any given community.

Keywords: density dependence, dispersal, ecological community, neutral model, spatial ecology, trade-off model.

* Corresponding author. Present address: Laboratoire d'Ecologie Terrestre, Centre National de la Recherche Scientifique, UMR 5552, 13 avenue du Colonel Roche, F-31029 Toulouse cedex 4, France; e-mail: chave@cict.fr.

† E-mail: helene@eno.princeton.edu.

‡ E-mail: slevin@eno.princeton.edu.

Many mechanisms have been proposed to explain the maintenance of species diversity within communities, one of the most fundamental questions in ecology (Hutchinson 1959; Levins 1970; May 1975; Pacala and Tilman 1993). These mechanisms shape community-level properties such as species-area curves, relative-abundance distributions, and spatial patterns of species occupancy. However, few studies have addressed the theoretical implications of diversity-maintaining mechanisms for community patterns.

These mechanisms can be broadly partitioned into "equilibrial" or "nonequilibrial." Equilibrial mechanisms can maintain constant species composition over time. They are based on functional differences among species in life-history strategy (Grubb 1977), habitat affinity (Ashton 1969, 1998), pests or predators (Janzen 1970; Connell 1971), and/or other factors that lead species to differ in their competitive ranking in differing circumstances as influenced by spatial and/or temporal heterogeneity. This heterogeneity can be exogenous (like topography), endogenous (the presence or absence of a particular competitor or pest), or both (light availability [Canham et al. 1994], soil fertility [Newbery and Proctor 1984], or disturbance regime [Connell 1979; Salo et al. 1986]). Nonequilibrial hypotheses, in contrast, explain diversity as a balance between speciation (or immigration) and extinction, with the species composition itself constantly changing (MacArthur and Wilson 1967; Caswell 1976; Simberloff 1976; Hubbell 1979; Chesson and Warner 1981). All these factors have been extensively discussed theoretically and tested in the field. They have all been shown to be capable of contributing to the maintenance of species diversity.

One way to test for the presence and importance of these factors in a given community is to examine community-level properties such as species-area curves, relative-abundance distributions, and spatial patterns in real

communities. Comparing them with the patterns found in model communities containing different combinations of the contributing factors should allow us to assess the relative magnitude of these mechanisms. The extensive data sets on species-area curves and relative-abundance distributions for many natural communities make this an appealing proposition. Yet relatively little work has been done on what patterns are expected under different mechanisms (Chave 2001). Thus, there is a need for theoretical work that clarifies which patterns are expected from which mechanisms and, thus, whether one can distinguish among mechanisms by looking at patterns.

Historically, most theoretical work on the species-area curve has been in the form of phenomenological models that are simply fit to data. This is in part because the term "species-area curve" has been applied somewhat indiscriminately to very different types of data (Holt 1992; Rosenzweig 1995). The two most common models are the Arrhenius power law $S = cA^z$ (Arrhenius 1921; Preston 1962; May 1975), which relates the number of species S and the area A, and the Fisher logarithmic law $S = \alpha \ln (1 + \rho A/\alpha)$, where ρ is the number of individuals per unit area (Fisher et al. 1943; Coleman 1981). Interestingly, the former model is well established in animal ecology (Wright 1981; Rosenzweig 1995), while the latter is more accepted in plant ecology (Condit et al. 1996; see Connor and McCoy 1979 and McGuinness 1984 for a discussion). Insofar as authors have attempted to derive the form of species-area curves, they have usually done so from assumptions about relative-abundance distributions and spatial patterns (Preston 1962) rather than by trying to explain all patterns from processes within communities. A quite different approach, which we build on here, consists of deriving these patterns from null models of biodiversity such as the models of Caswell (1976) or Hubbell (1995, 1997, 2001; Durrett and Levin 1996). Most recently, Buttel et al. (in press) have addressed a similar issue for an individual-based, spatially-explicit model with a competition-survival trade-off (Levins and Culver 1971; Horn and MacArthur 1972; Tilman 1994).

Theoretical work on species-abundance distributions has been based on deductive models. MacArthur (1960), Preston (1962), May (1975), and Sugihara (1980) proposed such models for the general form of species-abundance distributions. These were based on the idea that species partition a niche space. However, they provided no basis for explaining or predicting differences in relative-abundance distributions among communities. The exceptions, again, are studies exploring relative-abundance distributions in a null model (Hubbell 1997, 2001; Bramson et al. 1998).

Hubbell's (2001) nonequilibrium neutral model exhibits patterns that are strikingly similar to those observed in real communities. Whether these patterns are generic and potentially shared by other models or whether communities are actually neutral and nonequilibrium has been much debated (Connor and Simberloff 1979; Terborgh et al. 1996; Hubbell 1997; Ashton 1998). Yet, little theoretical work has been done to establish whether the presence, much less the strength, of equilibrium mechanisms such as niche differences or Janzen-Connell effects will change these patterns qualitatively (however, see Molofsky et al. 1999). Here, we provide the first broad comparison incorporating niche differences and other equilibrium, diversity-maintaining mechanisms using a framework of community models of sessile organisms competing for space. These models combine Hubbell's drift model (which is taken as the null, or neutral, model), interspecific variation in life-history strategy (niche differentiation), and conspecific density dependence (locally abundant species are disadvantaged). In future work, we intend to explore the importance of exogenous spatial and temporal variation in habitat and habitat specialization (e.g., topography, climate, soil, disturbance).

In this study, we investigated the implications of these mechanisms for community-level patterns. We tested the influence of the dispersal distance, the presence and strength of life-history niche differentiation, and the presence and strength of conspecific density dependence. We examined and compared species richness, species-area curves, relative-abundance distributions, and spatial patterns of some of these model communities. In addition to simulation results, we present exact analytical expressions for the variation of these patterns with community size. We also performed sensitivity analyses to establish that the results we obtain are general and not artifacts of the manner in which we implemented our simulations.

Model

General Framework

Our model is an individual-based, spatially-explicit model of a community of sessile organisms. The nature of the model makes it easy to change the dispersal, add life-history differences among species, and add conspecific density dependence. However, the addition of these differences also makes the model too complex to allow analytical treatment. Thus, most of our results are from simulations.

Landscape. Let the total model community at time t be composed of N_t individuals, each belonging to a given species $s \in \{1, \ldots, S\}$, with S the total number of species in the community. Each individual has a specific location in the landscape, which is a square lattice with L square

cells on a side (thus with L^2 cells total). At most one individual can occupy one square cell, and cells can be empty. We used periodic boundary conditions, which makes the landscape a torus; that is, sites on the right edge of the lattice are neighbors of those on the left edge, and cells on the bottom edge are neighbors of those on the top edge. This choice avoids spurious edge effects and best simulates a large community. Simulations were performed on large lattices, up to 4,096 × 4,096 cells in size, in order to avoid finite-size effects. In the context of a forest, one cell represents the area occupied by the canopy of a single adult tree, about 5 m × 5 m, much as in gap models such as those of Botkin et al. (1972) and Shugart (1984). For the intertidal, it represents the area occupied by an adult mussel (approximately 5 cm × 5 cm).

Births and Deaths. Each simulation starts with N_0 individuals representing S_0 species. In the absence of competition, an individual of species s dies at inherent mortality rate m_s, with $0 < m_s < 1$, and reproduces at rate f_s; that is, its inherent probability of death per time step is m_s, and the average number of offspring produced per time step is f_s. Each offspring is immediately dispersed from its parent to a new site according to one of the dispersal modes described below. If the site at which this propagule lands is occupied, it may or may not be able to take over from (and thus cause the death of) the current occupant. The death of individuals due to takeover by arriving propagules is not included in the inherent mortality rate m_s.

Speciation and Immigration. There is a small but steady input of new species in the system, which represents immigration of novel types and speciation; we will refer to it as simply speciation. A constant number of new species are introduced into the community at each time step. After Hubbell (1995), we designate this θ. Thus, the effective per capita speciation rate per time step is $\nu = \theta/N$. Each new species starts from a single individual (much as in macromutation), which is placed randomly on the model landscape.

Dispersal. The distances that offspring are dispersed have major effects on spatial patterns of species occupancy, on the frequency with which offspring disperse onto cells occupied by conspecifics, and, thus, on the level of interspecific competition. Dispersal distances are known to vary among communities, with long-distance dispersal for many intertidal communities (Thorson 1950; Caley et al. 1996) and relatively local dispersal in many terrestrial plant communities (Harper 1977; Willson 1993; Ouborg et al. 1999).

We examined the effects of four different kinds of propagule dispersal on community structure. At one extreme is global dispersal, in which all seeds are dispersed throughout the entire community. At the opposite extreme is nearest-neighbor dispersal, in which seeds are dispersed only to the four nearest neighbors of each cell. We also examined two intermediate types of dispersal. In one, seeds are dispersed according to a bivariate normal distribution, that is,

$$K_G(r) = \frac{r}{\sigma^2}\exp\left(-\frac{r^2}{2\sigma^2}\right), \tag{1}$$

where $K(r)dr$ is the probability that the propagule lands between distance r and distance $r + dr$ away from its parent and σ^2 is the mean squared dispersal distance. This function is a good fit to empirical seed shadows for short distances (e.g., Dalling et al. 1998). However, it is a poor fit far from the source (Willson 1993; Clark et al. 1999; Nathan and Muller-Landau 2000). Thus, our final type of dispersal employed a fat-tailed kernel (Kot et al. 1996). For this purpose, we used the dispersal kernel suggested by Clark et al. (1999), which takes the form

$$K_{2Dt}(r) = \frac{2pr}{u[1 + (r^2/u)]^{p+1}}, \quad p > 0, \tag{2}$$

where u and p are parameters determining the shape of the kernel. This function combines Gaussian dispersal at short distances with a power-law tail of long-distance dispersal.

Specific Models

Neutral Model. The first model we examine is a null, or neutral, model in which all species are identical. Strict neutrality, or equivalence of species, requires that all species have equal mortality rates, equal fecundities, and equal probability of their propagules taking over the sites on which they land, regardless of the identity of the previous occupant of the site, if any. For computational simplicity, we follow Hubbell (1997, 2001) and take as our neutral model one in which there are no empty sites, as deaths are always accompanied by births onto the same site. This corresponds to a system with saturating seed rain, in which all species have an inherent mortality rate of 1, fecundity is essentially infinite, and the probability of taking over occupied sites is 0. In this case, in each time step, there are L^2 successive deaths, chosen at random, each of which is immediately replaced (before the next death) by a new individual, the offspring of a neighboring site chosen according to the dispersal kernel. This corresponds to a system in which each time a tree dies, it is immediately replaced by the young of another tree in the community.

We chose the neutral model with no empty space for most comparisons because this scenario produces the fastest convergence to equilibrium and reduces the computational

time needed and because it makes the model easier to handle analytically. This neutral model is also known as the voter model with mutation (Clifford and Sudbury 1973; Durrett 1988), and its behavior with nearest-neighbor dispersal has been explored by Durrett and Levin (1996). If births and deaths are not always paired, then empty space appears in the system, and dynamics slow down. We have investigated the effects of the resulting empty space on patterns of diversity by examining models in which all species have nonzero inherent mortality rates, fecundity rates of 1, and takeover rates for propagules of 1.

The neutral model has a very interesting property, first pointed out by Holley and Liggett (1975): it admits a simple, dual representation, which provides an alternative route to understanding its behavior. The idea behind this dual representation is to fix a time t and to look for the "ancestors" of each site. Looking backward in time from time t, the set of ancestors of a site defines a path that gives the history of that site. A path ends where a speciation/immigration event took place. If, at a time $t' < t$, two paths meet at the same site, then the corresponding sites have the same ancestor and must therefore belong to the same species. A simple image of this process is a set of random walks, one per site at time t, that move backward in time and coalesce when they meet. Mutation corresponds to dead-end paths, and, if t is very large, the number of dead-end paths is simply the number of species in the community at time t. This method of investigating the model is much faster than ordinary simulations (J. Chave and E. G. Leigh, Jr., unpublished manuscript). Instead of running the simulations forward until an equilibrium is reached, this method essentially starts at the equilibrium and works backward, not to the very beginning but simply to the time of emergence of the longest-lived species present in the system at equilibrium. Because random walkers coalesce, we do not have to keep monitoring every site and its corresponding random walk; we only have to monitor the remaining walkers at time $t' < t$, a number that decreases very quickly. This allows for rapid numerical investigation of equilibrium forms of the species-area curve, relative-abundance distribution, and so forth, and it also permits analytical calculations, which prove intractable in almost any other spatially-explicit dynamic model. The analytical results presented here make extensive use of the dual representation algorithm.

Trade-off Models. While the neutral model provides an interesting null case, we know that there are many differences between species within real communities. If these differences result in a competitive hierarchy in which some species are always better than others, then they speed competitive exclusion (as modeled in Zhang and Lin 1997; Durrett and Levin 1998; Yu et al. 1998). However, when there are trade-offs such that no one species is best under all circumstances, differences between species can facilitate coexistence (Tilman and Pacala 1993). Such niche differences between species have been the focus of extensive ecological research and certainly influence the structure of communities. Thus, we investigate two models in which life-history trade-offs result in life-history niches that enhance coexistence; we refer to these as the trade-off models.

Both of the trade-off models we investigated incorporate an *r*-*K* trade-off between reproductive rate and competitive ability, in which species with lower reproductive rates are able to take over sites from species with higher reproductive rates (as in Hastings 1980; Tilman 1994). In our first model, the competition-survival trade-off model, species vary only in survival, while fecundity is constant at 1; thus, species with lower survival rates have higher competitive ability than those with higher survival. In real communities, such trade-offs between survival and competitive ability are often mediated by herbivores or predators. For example, fast-growing plant species are often more vulnerable to herbivores than slower-growing species that invest more in defenses (Crawley 1997), and larger-bodied, competitively dominant intertidal organisms experience higher risk of death by predation (Paine 1966). Our second model is the competition-fecundity trade-off model, in which species vary in fecundity but not mortality; species with lower fecundity outcompete those with higher fecundity. One example of such a trade-off between fecundity and competitive ability in plant communities is the trade-off between seed size and number. Smaller seeds can be produced in larger quantities, which increases the reproductive rate, but larger-seeded species are better competitors (Levin and Muller-Landau 2000).

These trade-off models have been the subject of extensive theoretical work, most of it on the behavior of the models when propagules are dispersed globally (Levins and Culver 1971; Horn and MacArthur 1972; Hastings 1980; May and Nowak 1994; Nowak and May 1994; Tilman 1994; Kinzig et al. 1999). Recent work shows that the competition-survival and competition-fecundity trade-off models have generically the same dynamic behavior under global dispersal (J. Dushoff, L. Worden J. Keymer, and S. Levin, unpublished results). Fewer studies have examined spatially-explicit versions with local dispersal (but see Buttel et al., in press); our own simulations suggest that the competition-survival and competition-fecundity trade-off models also behave similarly under local dispersal. Thus, we chose to use the competition-survival trade-off model for most of our results on local and global dispersal because it is computationally faster to implement; where not otherwise specified, "trade-off model" refers to the competition-survival trade-off model. We present results comparing the com-

petition-survival and competition-fecundity trade-off models to demonstrate the generality of our conclusions.

When speciation occurs in the trade-off model, reproductive rates of the new species are chosen so that the inverse of the reproductive rate is chosen from a uniform distribution. In the competition-survival trade-off model, new species are assigned a mortality drawn from a uniform distribution on [0, 1]. In the competition-fecundity trade-off model, new species are assigned a fecundity f_s, such that $1/f_s$ is drawn from a uniform distribution on $[1/F_{\max}, 1]$, where $F_{\max}$ is the maximum fecundity possible for a species. A finite $F_{\max}$ is necessary to achieve reasonable computational times.

Models with Conspecific Density Dependence. Another important equilibrium mechanism facilitating species coexistence is negative conspecific density dependence, in which an individual is disadvantaged where the density of conspecific adults is high. This may be due to the concentration of species-specific pests in such sites, so-called Janzen-Connell effects (Janzen 1970; Connell 1971), or, alternatively, to niche complementarity across species and thus heightened competitive effects of conspecific neighbors. There is extensive evidence for Janzen-Connell effects in tropical-forest tree communities (Condit et al. 1992; Hammond and Brown 1998; Harms et al. 2000), and there is some recent evidence for them in temperate forests (Packer and Clay 2000). Such Janzen-Connell effects give species a disadvantage when abundant and thus can powerfully influence species diversity. This influence was demonstrated mathematically by Armstrong (1989) for a nonspatial model with global dispersal. Molofsky et al. (1999) explored the effects of both negative (as here) and positive density dependence on the coexistence of two species in a spatially-explicit, individual-based model with nearest-neighbor dispersal.

We examined the effects of negative conspecific density dependence on both the neutral and trade-off models. In the simulations with density dependence, the probability of a propagule successfully establishing decreases in proportion to the number of neighboring sites occupied by conspecifics. We implement such effects by calculating the proportion q of the four nearest-neighbor cells of the cell at which the propagule lands that are occupied by conspecifics and letting the propagule escape density-dependent mortality with probability $w(q) = 1 - aq$, where a varies between 0 and 1 and determines the strength of the density-dependent effect.

Algorithms

The exact algorithms we used are given in appendix A.

Methods

Simulations Performed

To investigate the effects of trade-offs, density dependence, dispersal mode, and their interaction, we ran simulations for all combinations of the following: (*a*) full neutral model or competition-survival trade-off model (*b*) with or without density dependence for (*c*) nearest-neighbor dispersal, global dispersal, Gaussian dispersal with mean distance 1, 2, 4, 8, or 16 cell widths or Clark $2Dt$ dispersal (eq. [2]) with $p = 0.25$, 0.5, 1.0, 1.5, or 2.0. Most simulations were done on a large lattice of 1,024 × 1,024 cells ($L = 1{,}024$), with a speciation rate of 5×10^{-6} speciation events per site per time step. Some additional simulations were done on even larger lattices ($L = 2{,}048$ and $L = 4{,}096$) to assess finite-size effects. To allow time for the community to reach a dynamic equilibrium between speciation and extinction, we ran each model for 10^6 time steps. We said that the community had reached its equilibrium when there were no further directional changes in species number or the forms of species-area and relative-abundance curves. In the case of the neutral model, we checked our standard simulation results against results using the dual-representation algorithm to insure that the equilibrium had been reached.

Since the landscape generated by the competition-survival trade-off model contains considerable empty space while our standard neutral model has no empty space, we conducted additional runs to check for the influence of varying amounts of empty space in the neutral model itself. We ran the neutral model with fecundity 1, takeover probability 1, and inherent mortality rates of 0, one-sixteenth, two-sixteenths, and so on up to fifteen-sixteenths. These were done on 256 × 256 grids with a speciation rate of 9×10^{-4} per site per time step.

We compared the competition-fecundity and competition-survival trade-off models to test the influence of the form of trade-off. We used a maximum fecundity ($F_{\max}$) of 100 in the competition-fecundity trade-off model after verifying that our conclusions were insensitive to this parameter (simulations with $F_{\max} = 1{,}000$; results not shown). We ran the competition-fecundity model under different fixed mortality rates to find one at which the proportion of space occupied matched that in the competition-survival model; these runs were done on a small grid (256 × 256) and with a large speciation rate (9×10^{-4} per site per time step, or $\theta = 64$) to reduce computational time. We then ran large simulations for both models using the best mortality rate in the competition-fecundity model ($L = 1{,}024$ and $\theta = 5$ for both).

To examine how species richness and other patterns scaled with the size of the system, we ran simulations of the neutral and trade-off models without density dependence on lattices of side $L = 8$ to 1,024 cells. We held θ

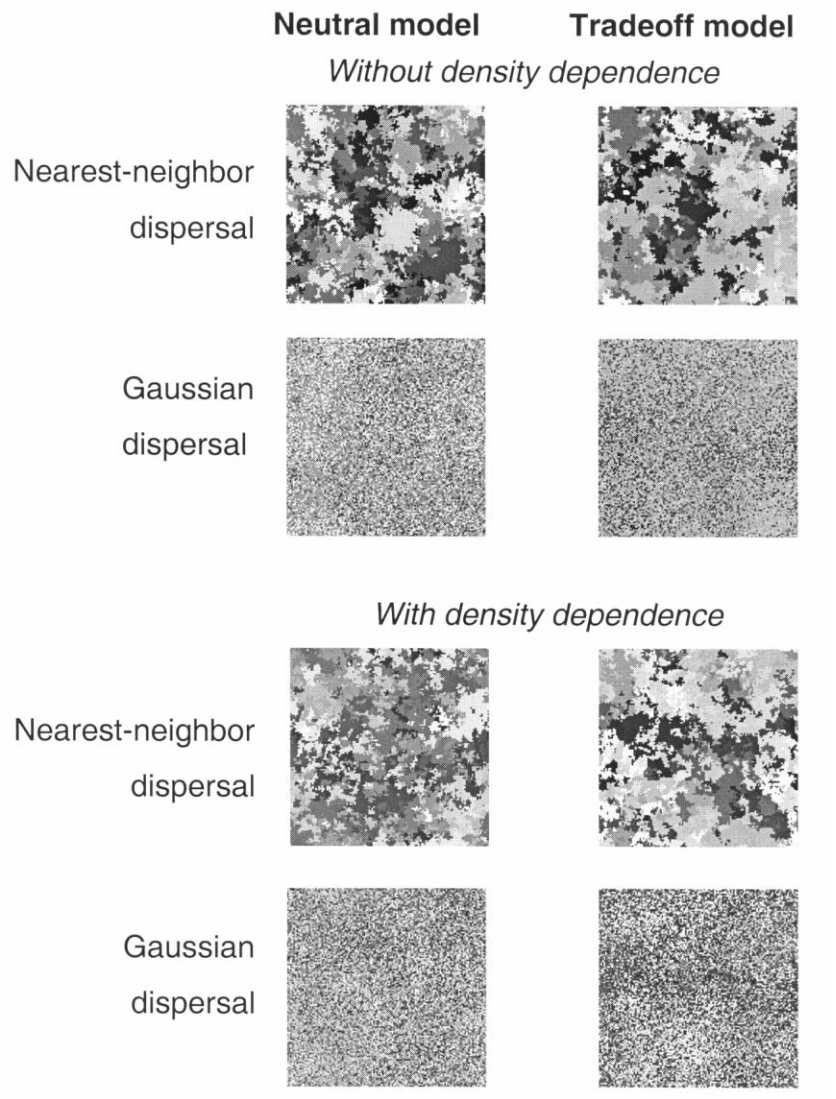

Figure 1: Spatial patterns of species occupancy after equilibrium has been reached in the different models: neutral and trade-off, with and without density dependence, under nearest-neighbor or Gaussian dispersal. Here, the neutral model is run with nonzero mortality rate so that the proportion of space occupied at any given time is the same as in the competition-survival trade-off model. The images depict the lattices on which the simulations took place, with each cell colored to match the identity of the species that occupied it most frequently over the previous 10 time steps. Each species having >10 individuals was randomly assigned a color; all other sites were colored white. The local-dispersal case depicted here is nearest-neighbor dispersal, while the long-distance dispersal case is Gaussian dispersal with $\sigma = 8$ (thus, the mean dispersal distance is 7.1 cell widths). Density dependence was implemented with $a = 0.4$. These simulations were run on a square lattice of side $L = 128$, with a speciation rate of $\theta = 2$.

(the number of new species per time step) constant at 5 for these runs; this effectively varied the per capita mutation rate, ν. Where available, analytical results are presented and compared with simulation results.

Patterns Recorded

In the simulation runs, we recorded the state of the model communities every 10 time steps. We focused on patterns whose form is robust across different implementations (see app. A) and that can be compared directly with field data, specifically species-area curves and relative-abundance distributions. Because these vary stochastically even after the dynamic equilibrium is reached, the equilibrium species-area and relative-abundance curves that we report are averages over at least 10 curves recorded 1,000 time steps apart after equilibrium was attained. For the neutral model, simulations and comparison with the dual repre-

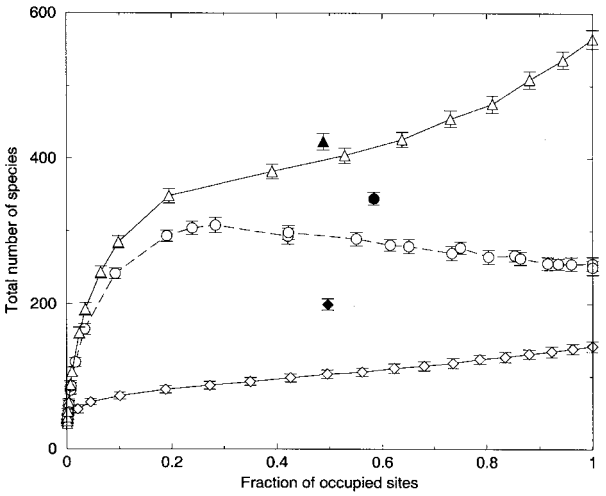

Figure 2: The equilibrium number of species and the fraction of sites occupied in the neutral model under different mortality rates (*open symbols*) compared with the number of species in the corresponding competition-survival trade-off model (*filled symbols*). Shown here are nearest-neighbor dispersal with density dependence (*triangles*), nearest-neighbor dispersal without density dependence (*circles*), and global dispersal without density dependence (*diamonds*). For all simulations, $L = 256$ and $\theta = 64$. For the cases with density dependence, $a = 0.4$. Mean number of species and standard error (*error bars*) were computed from 50 simulations.

sentation algorithm revealed that equilibrium was reached at around $T_{eq} \approx L^2/2$ time steps, that is, around 5×10^5 time steps for $L = 1{,}024$. We also examine the spatial patterns of site occupancy, which illuminate the mechanisms behind the different species-area curves and relative-abundance distributions.

We constructed species-area curves using the bisection procedure (Greig-Smith 1952; Whittaker 1972). Each point on these curves represents the average number of species in disjoint (nonoverlapping) quadrats of that area that together completely cover the simulation grid. This curve shows how species number changes as the sample size changes within a given community (Condit et al. 1996).

We analyzed relative-abundance distributions for the whole community and for square subsets of it. We display these distributions both as rank-abundance curves and as histograms of the number of species in different abundance classes (species-abundance distribution).

Robustness

Many of the features of the model could be implemented in different ways that have somewhat different biological parallels but arguably still represent the same general phenomena. We examined whether a number of such variations affected the qualitative results that we compare across models. The details of the tests we performed and their results can be found in appendix A.

Results

Spatial Patterns

The models differ substantially in the proportion of sites occupied and in the degree to which members of the same species are clumped. These differences, in turn, drive differences in the species-area curves and the relative-abundance distributions. In the competition-survival trade-off model, approximately half the sites are empty at any given time because the inherent mortality rates in this model are necessarily nonzero for most species. This contrasts with occupancy of all sites under the neutral model with no mortality. To illuminate the differences in species clustering between the competition-survival trade-off model and the neutral model without the additional complication of the difference in empty space, we compared this trade-off model with a neutral model with a nonzero mortality rate chosen so that the proportion of space occupied was the same in both models. We then examined the spatial patterns when each site is assigned the identity of the species that occupied it most frequently over the previous 10 time steps, thus eliminating empty space from the picture (the empty space makes it harder to see the patterns in species clustering).

The equilibrium spatial patterns are most strongly affected by dispersal distance and density dependence, while they seem relatively little affected by the presence or absence of trade-offs between species (fig. 1). Distributions of species are much more clumped and species richness is higher under local (nearest-neighbor) dispersal than under longer-distance dispersal, even though the long-distance dispersal depicted here is not that long ($\sigma = 8$, mean dispersal distance 7.1 cell widths, median 6.7, ninety-ninth percentile 17.2). Models with density dependence show much smaller clumps, and higher species richness, than those without density dependence, especially in the neutral model. Overall, spatial patterns are relatively similar between the neutral and the trade-off model; however, the trade-off model is less sensitive than the neutral model to the influence of changes in dispersal and density dependence. There are also more rare species (represented by <10 individuals and colored in white in fig. 1) in the neutral model than in the trade-off model.

Species Richness

Species richness was much higher under local dispersal than under global dispersal, higher with density dependence than without, and higher in the competition-

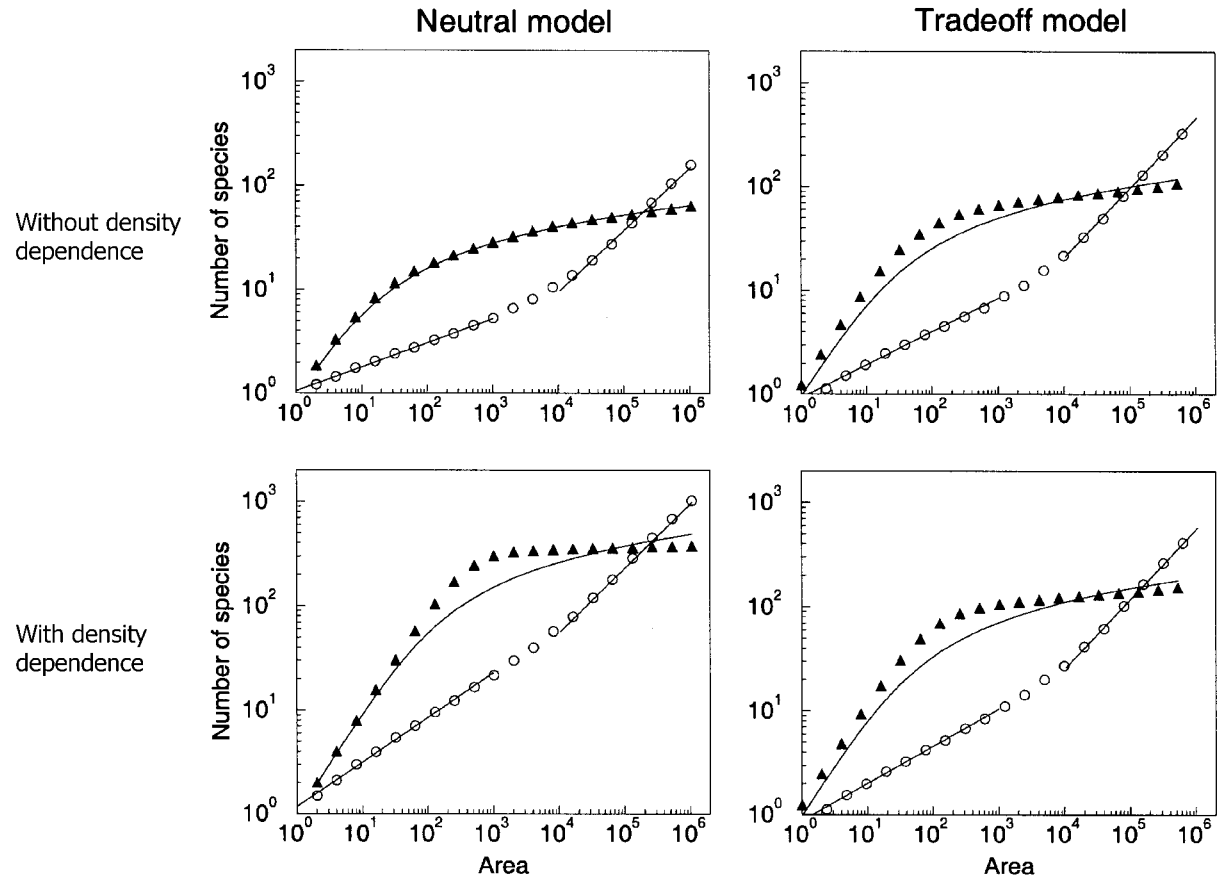

Figure 3: The equilibrium species-area curves in the different models: neutral model without density dependence (*top left*), trade-off model without density dependence (*top right*), neutral model with density dependence (*bottom left*), and trade-off model with density dependence (*bottom right*). To better compare these curves, we plotted the occupied area along the *X*-axis (i.e., the number of individuals in the community). In each plot, the species-area curves (SACs) obtained with two extreme dispersal kernels are shown: nearest-neighbor dispersal (*open circles*) and global dispersal (*filled triangles*). The SACs with nearest-neighbor dispersal were fitted by two power laws (for small and large scales). The fitted parameters are given in table 1. The SACs with global dispersal were fitted by Fisher's law, and we found the following: *top left*, $\alpha = 5.29$ ($r^2 = 0.996$); *top right*, $\alpha = 11.0$ ($r^2 = 0.86$); *bottom left*, $\alpha = 49.2$ ($r^2 = 0.76$); *bottom right*, $\alpha = 17.4$ ($r^2 = 0.79$). Each curve was constructed from the average of 10 SACs recorded 1,000 time steps apart after equilibrium was reached in simulations with $L = 1{,}024$, $\theta = 5$, and (where applicable) $a = 0.1$.

survival trade-off model than in the neutral model when controlling for differences in the proportion of space occupied. The equilibrium species richness in the neutral model changed modestly when the mortality rate was changed. For global dispersal, the number of species declined as the mortality rate increased and the proportion of occupied sites declined; for local dispersal, the number of species first increased and then decreased (fig. 2). Species richness in the trade-off model was always higher than that in the neutral model when both systems had the same proportion of sites occupied (fig. 2). (This occurred at a mortality rate of approximately 0.62 for global dispersal without density dependence, 0.44 for nearest-neighbor dispersal without density dependence, and 0.42 for nearest-neighbor dispersal with density dependence.) For global dispersal without density dependence, the difference in species number between the trade-off and neutral models was larger when compensating for the difference in site occupancy; for local dispersal without density dependence, it was smaller (but still significant). Most notable, for nearest-neighbor dispersal with density dependence, species number is higher in the trade-off model than in a neutral model with an equivalent amount of empty space, whereas it is lower than the species richness in the neutral model with no empty space (zero mortality).

Species-Area Curves

The shape of the species-area curve (SAC) is strongly affected by dispersal distances but is not much affected by

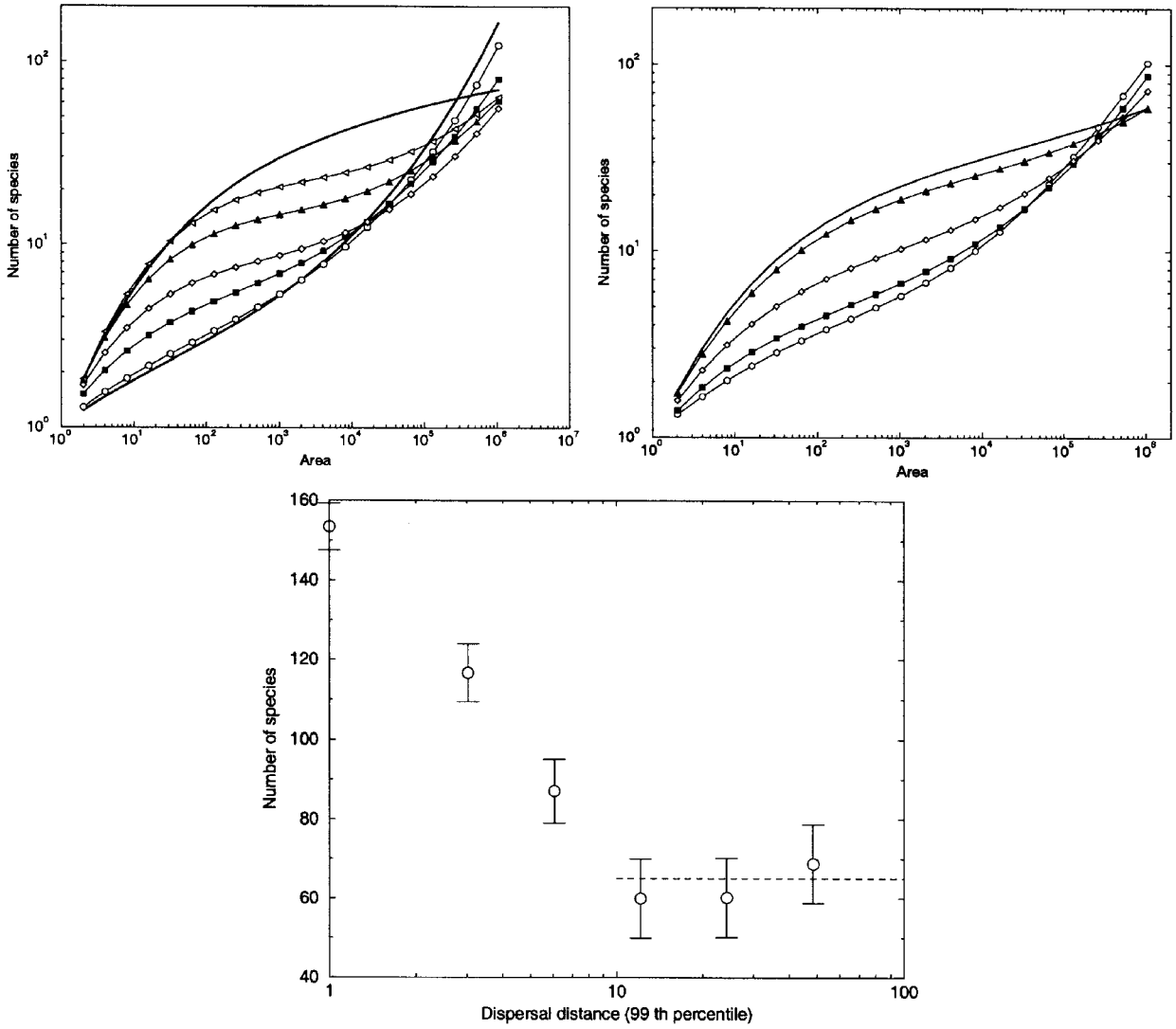

Figure 4: *Top panels*, the equilibrium species-area curves (SACs) in the neutral model without density dependence for different kinds of distances of dispersal (averages over 10 runs). *Top left*, the plain solid lines are the nearest-neighbor and global-dispersal SACs (cf. fig. 3). In between, the lines display curves for Gaussian dispersal kernels with $\sigma = 1$ (*open circles*), 2 (*filled squares*), 4 (*open diamonds*), 8 (*filled triangles*), and 16 (*open triangles*). *Top right*, SACs achieved under the fat-tail dispersal kernel (eq. [2]), with $u = 1$ and $p = 0.25$, 0.5, 1.0, 1.5, and 2.0 (from top to bottom). *Bottom panel*, mean and standard deviation of the total number of species as a function of the ninety-ninth-percentile dispersal distance ($=3.03\sigma$). The dashed line shows the number of species in the global-dispersal scenario. All simulations with $\theta = 5$, $L = 1{,}024$, and (when applicable) $a = 0.1$.

other factors (fig. 3). On a log-log scale, the SACs of models with nearest-neighbor dispersal are convex, while those of global dispersal are concave. Models with intermediate types of dispersal have SACs with intermediate shapes (fig. 4).

The global-dispersal SACs are fairly well fit by Fisher's law,

$$S(A) = \alpha \ln\left(1 + \frac{\rho A}{\alpha}\right), \tag{3}$$

in all cases ($N = \rho A$). For the neutral model without density dependence, Fisher's law is actually the exact solution (Coleman 1981; Bramson et al. 1996), and our simulations

Table 1: Best power-law fits ($S = cA^z$) to the species-area curves shown in figure 3 of models with nearest-neighbor dispersal for small ($1–10^3$) and large ($10^4–10^6$) areas

	Neutral model		Trade-off model	
Range	c	z	c	z
Without density dependence:				
$1–10^3$	1.06	.23	.92	.32
$10^4–10^6$	.037	.60	.043	.67
With density dependence:				
$1–10^3$	1.17	.43	.90	.36
$10^4–10^6$	.18	.62	.053	.67

Note: All the fits were highly significant ($r^2 > 0.99$). The measured slope at large scales is not 1 due to our choice of toroidal boundary conditions; the maximal area used in our fits is one-fourth of the total simulated area (see text).

clearly confirm this result. For all the other scenarios, the best-fit Fisher's law underestimates the species richness at medium scales and overestimates it at large scales.

On a log-log scale, it appears that the nearest-neighbor SACs are well fit by two straight lines, with one well-defined slope up to $10^3–10^4$ and another, steeper slope beyond this scale (table 1). However, if we calculate the slopes (z) of the log-log plots,

$$z(A) = \frac{d\ln(S)}{d\ln(A)}, \tag{4}$$

and plot these as a function of area, we can easily see that the curves deviate substantially from this assumption (fig. 5). Note that the dip in the z exponent at the largest scales of the model is a result of the toroidal landscape structure. On a torus, as additional area is added to a subset; eventually, that added area becomes closer to the starting point because the landscape wraps around. Thus, that area becomes more similar to the area already in the sample, and fewer new species are added. This effect occurs at scales beyond half the length of the system and thus beyond one-quarter of the area. On a landscape that does not have such periodic boundaries, this effect would disappear; the z values would continue to increase, approaching 1 for all local-dispersal scenarios (results not shown).

Density dependence has a very strong positive effect on species number in the neutral model, especially when dispersal is local (a 10-fold increase with a density dependence of strength $a = 0.4$). It also affects the shape of the curve, making the global-dispersal curves more concave and the local-dispersal curves somewhat less convex (fig. 3). The neutral and trade-off models show relatively similar patterns.

We analyzed the variance of the SACs in detail for the neutral model. For any particular SAC, the standard deviation of species in a given area varies in proportion to the mean number of species in that area so that the coefficient of variation is essentially constant for all areas A within a given SAC. Between simulations, the number of species and the standard deviations varied depending on dispersal distances, with smaller species numbers and larger standard deviations for longer dispersal distances.

Rank-Abundance and Relative-Abundance Distributions

The distribution of relative abundances for the entire community is affected primarily by dispersal type and secondarily by density dependence (figs. 6, 7). The rank-abundance curves of nearest-neighbor models are S-shaped on log-linear plots, while those of global-dispersal models are entirely concave, with the exception in both cases of the neutral model without density dependence; under those conditions, the curves are nearly straight lines (fig. 6), and thus the histogram of relative abundances is nearly flat (fig. 7). The addition of density dependence and the presence or absence of trade-offs greatly increases the number of species with moderate abundances, which leads to flatter rank-abundance curves (fig. 6) and to a unimodal histogram of relative abundances (fig. 7). The addition of trade-offs has a similar, but less pronounced, effect. When we examine the distribution of relative abundances in subsets of the community, we find that shapes remain qualitatively the same under global dispersal, as they should. However, under local dispersal, the distribution of relative abundances becomes more lognormal, and the rank-abundance distribution linear and more S-shaped, as smaller subsets are taken (shown for the neutral model without density dependence in fig. 8). Thus, in subsets, which are closer to the kind of data most often collected empirically, the relative-abundance distributions of all the communities are qualitatively more similar.

For the neutral model with global dispersal, it is possible to prove that the relative-abundance distribution for the full community must have the observed form. Let $p_i(t)$ be the fraction of individuals belonging to species i at time t. The unit segment [0, 1] is partitioned into S domains of size p_i, which change in size through time. It is convenient to look only at the boundary between two domains; they perform random walks on the segment [0, 1], and a species goes extinct when two such random walks meet (when the boundaries coalesce). The appearance of a new species is equivalent to a "branching" of a boundary, which gives rise to a new domain of size $1/N$. This representation allows one to prove rigorously (Ben Avraham et al. 1990) that the rank-abundance curve is an exponential function, $N(\text{rank}) = \exp(-\text{rank}/\theta)/\theta$, and thus the histogram of relative abundances is flat.

The histograms of relative abundances for all the other

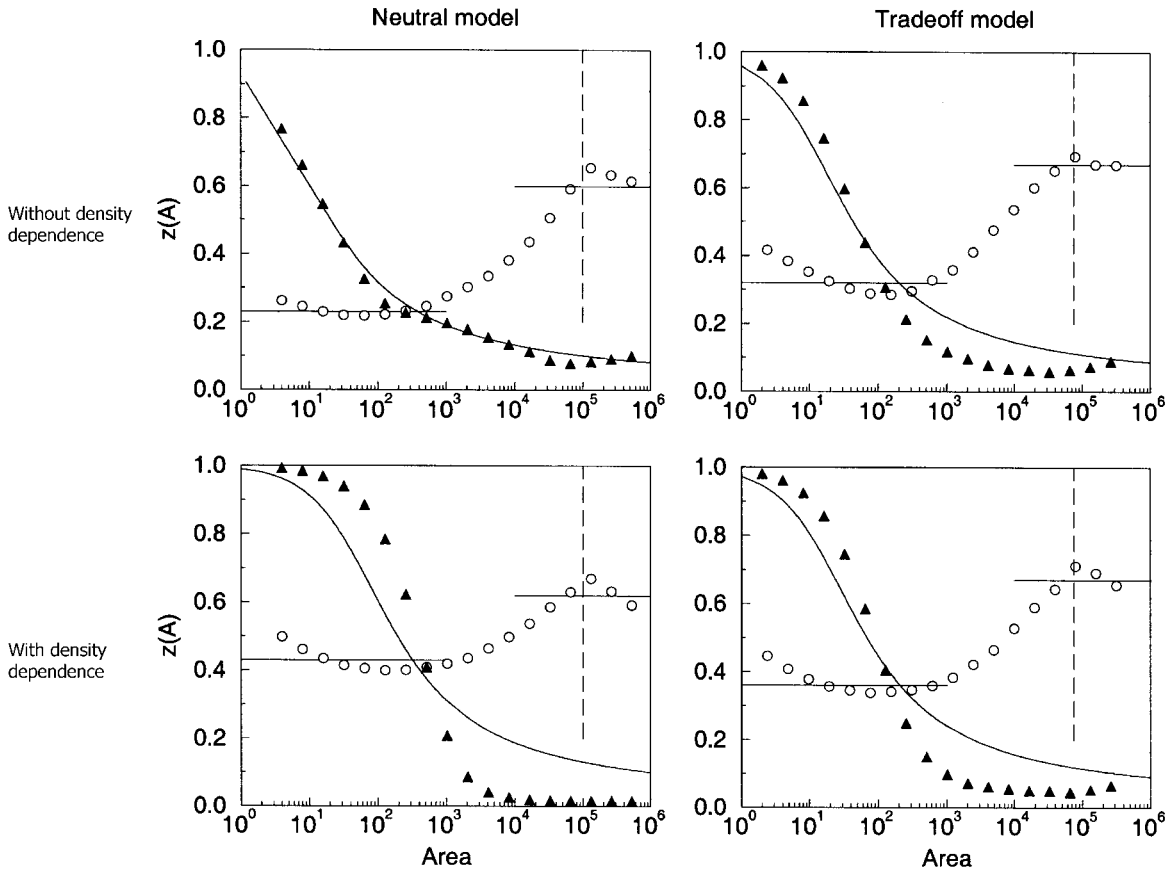

Figure 5: The z exponent of the species-area curve shown in figure 3 computed as the slope of the log-log plots for the neutral model without density dependence (*top left*), trade-off model without density dependence (*top right*), neutral model with density dependence (*bottom left*), and trade-off model with density dependence (*bottom right*). Open symbols depict nearest-neighbor dispersal, and filled symbols depict global dispersal.

models, as well as for subsets of the neutral model, are unimodal and skewed toward rare species. They have more rare species than Preston's canonical lognormal distribution of relative abundances (Preston 1962), which is expected to arise in the case of a large number of sources of environmental heterogeneity (May 1975). Like Preston's distribution, they have an S-shaped rank-abundance curve.

Comparison of the Trade-off Models

The two trade-off models produced almost identical species-area curves and abundance distributions under nearest-neighbor dispersal after controlling for the proportion of space occupied (fig. 9). In the competition-fecundity trade-off model, species richness depended on the proportion of space occupied, which varied with the mortality rate (fig. 10). Small-scale simulations showed that the competition-fecundity model with a mortality rate of $m \simeq 0.7$ had similar amounts of empty space compared with the competition-survival model; thus, this is the mortality rate that was used for the larger run, the results of which were compared with those previously obtained for the competition-survival model (fig. 9).

Finite-Size Scaling

Because our model communities are small compared with real communities and have unrealistically high speciation rates, it is critical to understand how our results scale with community size and speciation rate (Durrett and Levin 1996). We are particularly interested in how total species richness S scales with the number of individuals in the system N, the speciation rate θ, and the dispersal distance σ. That is, we would like to find the form of the function

$$S = F(N, \theta, \sigma).$$

We refer to this function F as a scaling function. It can

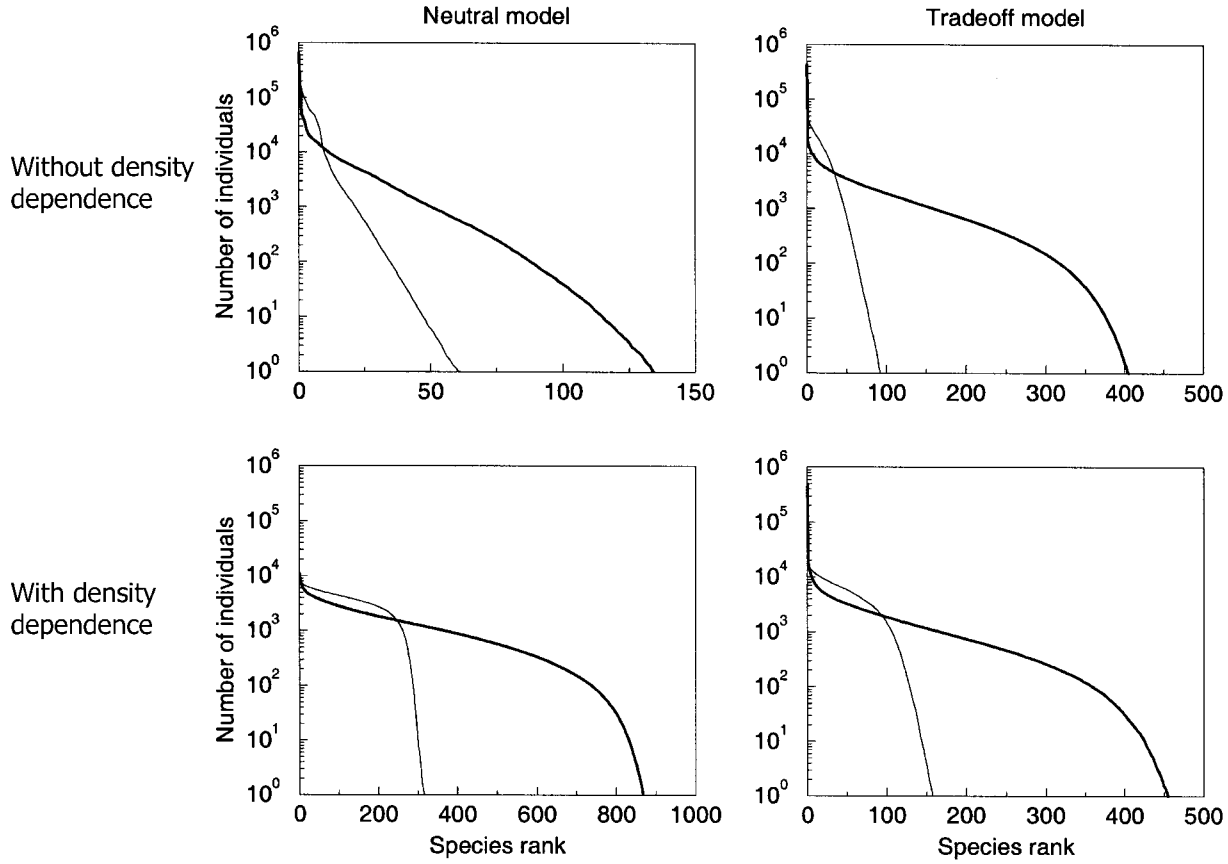

Figure 6: Equilibrium rank-abundance curves for the different models: neutral model without density dependence (*top left*), trade-off model without density dependence (*top right*), neutral model with density dependence (*bottom left*), and trade-off model with density dependence (*bottom right*). Bold curves correspond to the model with nearest-neighbor dispersal, while simple lines correspond to global dispersal. All simulations with $\theta = 5$, $L = 1{,}024$, and (when applicable) $a = 0.1$.

be thought of as a species-area relationship that relates number of species to number of individuals; however, it has a qualitatively very different interpretation from the standard SAC, since here it is total number of individuals in the entire community, rather than the number of individuals in the sample, that varies.

Neutral Model. Bramson et al. (1998) obtained exact expressions for the scaling function F for the neutral model, also known as the multitype voter model with mutation. In appendix B, we provide their fundamental theorem, which we use to find the function F for any N, θ, and σ. This theorem relates the function $F(N, \theta, \sigma)$ to the properties of a simple random walk in two dimensions of space. Namely, it relates $F(N, \theta, \sigma)$ with the number of distinct sites visited by a random walk with variance σ, $V_\sigma(t)$. A rigorous proof of this result is given in Bramson et al. (1998).

Under global dispersal, the random walk essentially performs long jumps, visiting a new site each time step, and thus $V(t) \approx t$. Making use of equation (1), we find

$$\overline{F}(N, \theta, \sigma) \simeq \theta \ln (N). \tag{5}$$

This result is classic in ecology (Fisher et al. 1943; Coleman 1981). It has been repeatedly derived using the Ewens formula in the past (Ewens 1972; Watterson 1974; Caswell 1976; Hubbell 1997). In the case of nearest-neighbor dispersal in a two-dimensional lattice, we have $\overline{V}(t) = \pi t / \ln (t)$ (Dvoretzky and Erdős 1951), and thus,

$$\overline{F}(N, \theta, \sigma) \simeq \frac{\theta}{2\pi\sigma^2} [\ln (N)]^2, \tag{6}$$

as proved in Bramson et al. (1998). In appendix B, we provide some additional information on the variance of $F(N, \theta, \sigma)$.

The result in equation (6) breaks down as the variance

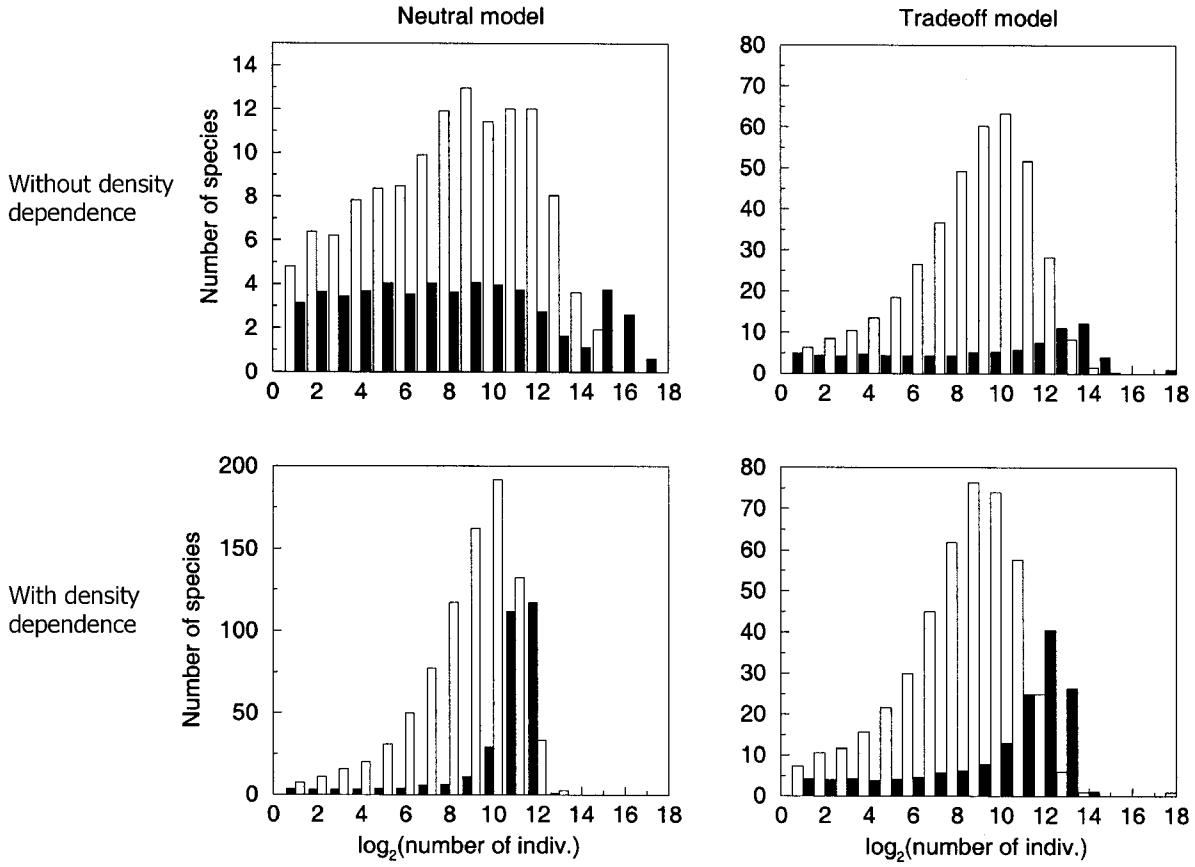

Figure 7: Equilibrium species-abundance distributions for the different models: neutral model without density dependence (*top left*), trade-off model without density dependence (*top right*), neutral model with density dependence (*bottom left*), and trade-off model with density dependence (*bottom right*). Open bars correspond to the model with nearest-neighbor dispersal, while filled bars correspond to global dispersal. Simulation parameters as in figure 6.

of the dispersal kernel approaches the size of the system ($\sigma \approx L$), which makes dispersal effectively global. The variance of the fat-tail dispersal kernel of equation (2) is finite for some parameter values but not others, and thus the shape of the scaling function varies. For $p > 1$, the variance is finite, and equation (6) holds. For $0 < p < 1$, the variance is infinite, although the dispersal kernel remains defined. In this case, however, the value of $V_{p,u}(t)$ is known analytically (cf. Gillis and Weiss 1970 and app. B). For $p <$ 1, the scaling function behaves like that of a system with global-dispersal kernel, and formula (3) holds.

We verified the analytical results given in these formulas using numerical simulations (fig. 11). Note that the scaling function for the global-dispersal case was better fit by Fisher's law (3) (fits shown in fig. 11) than by the asymptotic formula (5) (fits not shown).

Trade-off Models. There is no theory available for the scaling function $F(N, \theta, \sigma)$ of the trade-off models. Buttel et al. (in press) have found numerically, however, that the scaling function of the competition-survival trade-off model follows the power-law form $S = cA^z$, with $z \simeq 0.17$ for the global-dispersal case and $z \simeq 0.34$ for nearest-neighbor dispersal. Our simulations confirm this intriguing result (fig. 11).

Discussion

Understanding the Mechanisms

The three mechanisms examined here—dispersal limitation, life-history niche differentiation, and conspecific density dependence—all can contribute to the maintenance of species richness. Each fundamentally increases the strength of intraspecific competition and decreases the strength of interspecific competition, thus making each species more limited by its own kind than by others. Yet the mechanisms are not equivalent. The coexistence facilitated by local dispersal alone is little more than a slow-

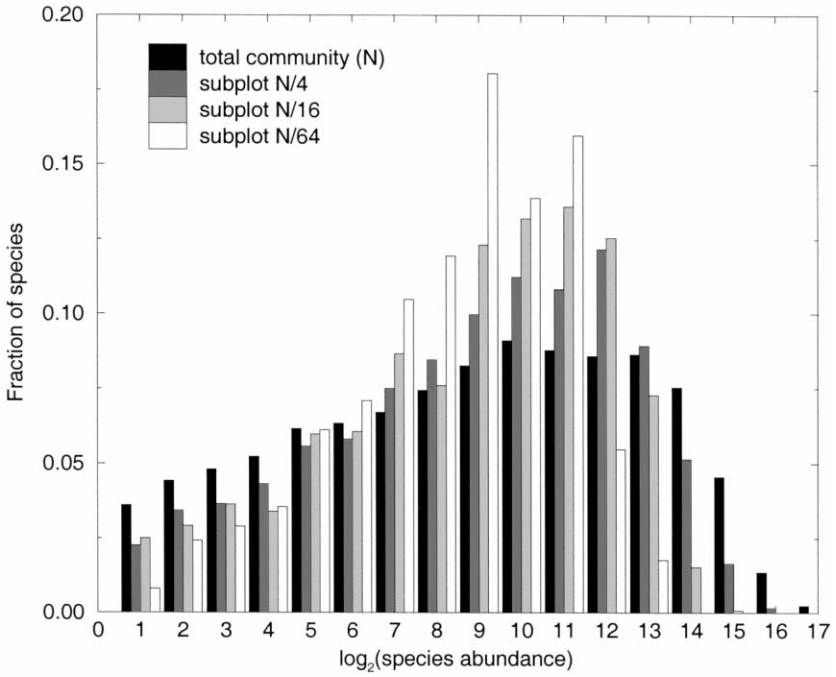

Figure 8: Equilibrium relative-abundance distributions of different-sized subplots for the neutral model with nearest-neighbor dispersal and without density dependence. The relative-abundance distribution of the total community with N individuals is compared to square subsets of the community that are one-fourth, one-sixteenth, and one-sixty-fourth the total area. Relative abundances (proportion of all individuals) rather than absolute abundances are presented to make their comparison easier. The mode is more marked for small subcommunities than for the entire community, and the number of rare species is comparatively smaller. Here, $L = 1{,}024$ and $\theta = 5$.

ing of the speed with which species drift to extinction, as they inevitably must, balanced by speciation or invasion of new species (Durrett and Levin 1994). There is no robustness to this coexistence, no stable equilibrium value to which the abundance of any species tends to return. By contrast, both niche differences and density dependence result in communities that show robustness to perturbation, with equilibrium abundances for individual species to which the populations will tend. For the density-dependent case, these equilibrium abundances are equal across all species when there is no dispersal limitation (Armstrong 1989). For the trade-off model, equilibrium abundances are determined by the array of reproductive rates in the community and vary among species (Nowak and May 1994; Kinzig et al. 1999).

The scale of dispersal has a huge effect on the number of species maintained in the system in all the models (for a similar result in the context of the neutral model, see Hubbell 2001, chap. 7). Under local dispersal, individuals of the same species are clumped together, which results in patchy spatial distributions. Because a large proportion of propagules land on sites occupied by neighbors of the same species, intraspecific competition is stronger than interspecific competition, and potential rates of increase and decrease in abundances of species are reduced (Pacala and Levin 1997). Founder effects dominate, which determines which species is present where. At small scales, the SAC first rises steeply (the first individual always represents one species) and then takes a lower slope as it saturates to some degree on local species richness. At sufficiently large spatial scales relative to the distance of dispersal, the curve again rises steeply because there is complete isolation, with essentially no exchange of propagules. Thus, at large scales, we have locally unique species, and the SAC has a slope of 1 (proven in the limit of infinite system size by Bramson et al. [1996]; see also Durrett and Levin 1996). Under global dispersal, in contrast, what is anywhere is everywhere, and thus the spatially-explicit information becomes irrelevant. The number of species that can be packed in the community rises only as the logarithm of the community size. The rank-abundance curve is exponential (Caswell 1976), and the histogram of relative abundances is relatively flat.

A decrease in the proportion of occupied cells simultaneously decreases the total number of individuals in the community and decreases the effective dispersal distance. Therefore, species richness may increase or decrease as the mortality rate increases. The decrease in the total number

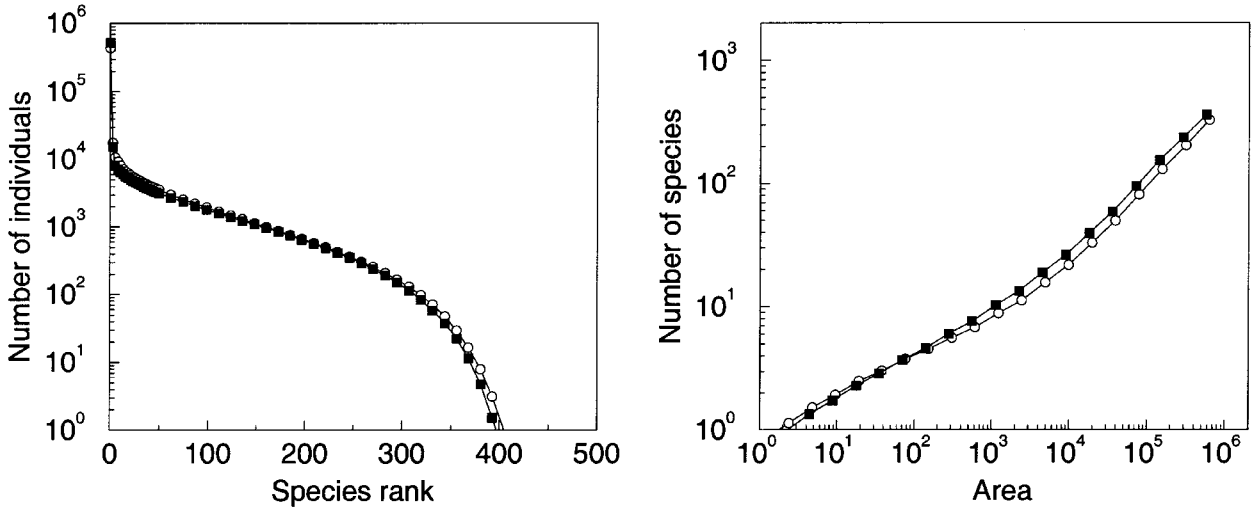

Figure 9: Rank-abundance curves (*left*) and species-area curves (*right*) for two versions of the trade-off model: the competition-survival model (*open circles*) and the competition-fecundity model with a mortality rate set to $m = 0.7$ and maximum fecundity $F_{max} = 100$ (*filled squares*). Both models gave very similar results. All simulations with $L = 1{,}024$ and $\theta = 5$.

of individuals acts to reduce the total species richness. At the same time, the distance to the next occupied cell increases on average, which makes the scale of dispersal in local-dispersal models smaller relative to the scale of interindividual distances. This increases intraspecific clumping and reduces interspecific interaction, thereby enhancing species richness. Under global dispersal, it is the decline in community size alone that is evident (the scale of dispersal remains the same), and thus species richness always declines as the proportion of empty sites increases.

Life-history niche differences decrease interspecific competition because, on average, only those propagules landing on sites occupied by individuals from species with higher reproductive rates are successful. Indeed, we can think of sites as experiencing succession from higher to lower reproductive rates, with succession continually interrupted (reset) by mortality or disturbance. Species with a high reproductive rate do best early in succession; they have a better chance of colonizing empty sites. Species with a low reproductive rate have an advantage late in succession, when they are the only ones who can take over sites. Each species has a carrying capacity or equilibrium abundance determined by the relative abundance of its favored habitat and by its own reproductive rate (Nowak and May 1994; Kinzig et al. 1999). Species richness is thus maintained by the presence of successional niches of species (Pacala and Rees 1998) and by the phase differences between sites in their successional status (Levin 1976). Nevertheless, the SACs of the trade-off models are essentially identical to those for the neutral models with the same dispersal types. The relative-abundance distributions, however, are different. There are fewer very abundant or very rare species, which reflects the influence of the species-specific equilibrium abundances and the resulting directional pressures on species abundances.

With density dependence, individuals explicitly depress the success of their conspecifics, which increases the competitive effect of conspecifics relative to individuals of other species. In a sense, space becomes a mosaic of different habitats. For each species, the local density of conspecifics determines suitability.

Because locally common species are at a disadvantage, conspecific clusters are broken up, and richness—both local and global—is elevated. This effect is particularly pronounced in local-dispersal models, where clumping would otherwise be strong. The SACs are uniformly higher than in models without density dependence; their general shapes remain determined by dispersal and are unchanged. Because common species are at a disadvantage and rare ones at an advantage and because the equilibrium abundances are equal and intermediate, the relative-abundance distribution shows a larger proportion of species at intermediate abundances.

Connections to Real Communities

The simulations reported here were unrealistic in many respects. However, we argue that the general results apply to a wide range of more realistic—but more computationally difficult to simulate—model communities. The

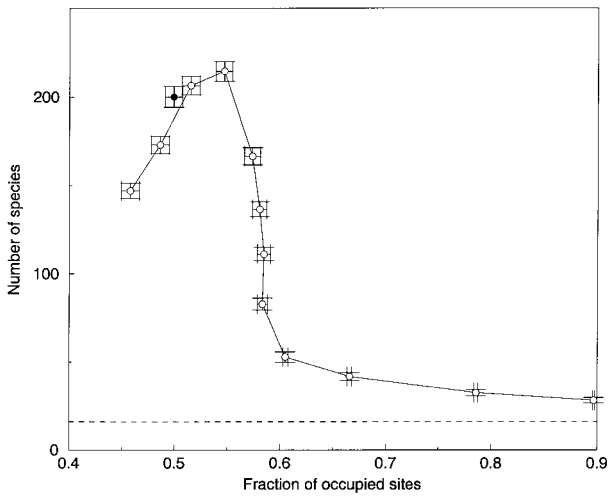

Figure 10: The species richness and the fraction of sites occupied in the competition-survival trade-off model (*filled circle*) and in the competition-fecundity trade-off model under various mortality rates (*open circles*) in the amount of space occupied and in species richness. All simulations with nearest-neighbor dispersal and $\theta = 16$. Mortality rates in the competition-fecundity trade-off model are (from left to right) $m = 0.9$, 0.8, 0.7, 0.6, 0.55, 0.5, 0.45, 0.4, 0.35, 0.3, 0.2, and 0.1.

trade-offs we examine here are not the only, or even the most important, ones among species in natural communities, but we believe the patterns common to the two trade-offs we do examine are indicative of how communities are affected by niche differences in general. The proportion of space occupied in the competition-survival trade-off model is low (perhaps unrealistically so), but qualitatively, the same dynamics are observed in a competition-fecundity model in which nearly all spaces are filled (May and Nowak 1994); indeed, the dynamics are quantitatively identical as well when system size and dispersal distance are properly scaled by the amount of space occupied. Janzen-Connell effects that lead to conspecific density dependence obviously occur on scales larger than simply the four nearest neighbors and affect more than just the probability of establishment. However, their effects on community patterns will be qualitatively the same as long as they have the same strength across all species (e.g., Armstrong 1989). Clearly, the simulated communities are unrealistically small, and the speciation rate is unrealistically large. However, our simulations across a range of system sizes and speciation rates establish that the qualitative patterns are the same and that the total species numbers scale simply. Further, our finite-size scaling analysis shows that the number of species in the total community of arbitrarily large size can be deduced from information on smaller systems.

The results here suggest that the scale of dispersal is the most important factor in determining the shapes of SACs and the only one about which conclusions can be drawn from the shapes of observed curves. More specifically, the important question is the speed of dispersal relative to the speciation rate; these together define the correlation length of the system (Durrett and Levin 1996). Actual species-area curves for tropical forest plots up to 50 ha in size (Condit et al. 1996) show the concavity—and even much the same curve for changes in z values across scales—that we observed in models with global or fat-tailed dispersal (figs. 3–5), which suggests that dispersal is relatively homogenizing even at the 1-km scale. However, accounting for the clumping of conspecific individuals leads to a systematic improvement in fitting these SACs relative to models assuming random placement (effectively global dispersal; Coleman 1981); this implies that local dispersal is important in shaping these patterns (Plotkin et al. 2000*a*, 2000*b*). Overall, intermediate dispersal distance distributions with median dispersal distances of 35 m produce the best fit to the SAC, capturing the small-scale clumping and the overall mixing within a 50-ha plot of tropical rain forest (Hubbell 2001). On larger scales, interprovincial species-area curves that combine data from separate biogeographic regions have slopes near 1, which is consistent with the fact that they exchange virtually no individuals (Rosenzweig 1995). As Hubbell (2001) points out and as our results confirm, local dispersal alone can explain the triphasic structure of species-area curves: steep at small scales, then shallower, and finally steep again across provinces. Our results with intermediate propagule dispersal confirm this claim. This pattern holds for all models we examined that had local dispersal, including those that are not neutral.

Empirical relative-abundance distributions are most often approximately lognormal, with an excess of rare species (Hubbell 2001). This pattern is present in all the models having local dispersal and is most pronounced in the neutral model. The models with density dependence show an unusual degree of evenness in abundances, with most species having similar intermediate abundances. This suggests that most real communities do not exhibit the sort of density dependence modeled here, one that is identical in strength across all species. Future work should examine not only the shape of abundance distributions within an area but consistency in abundances of individual species across regions (Rabinowitz 1981; Pitman et al. 1999). For example, intersite similarity in species composition at the landscape scale (Ashton and Hall 1992; Terborgh and Andresen 1998; Pitman et al. 1999) has recently been compared with that expected under the neutral model (R. Condit, N. Pitman, J. Chave, et al., unpublished manuscript).

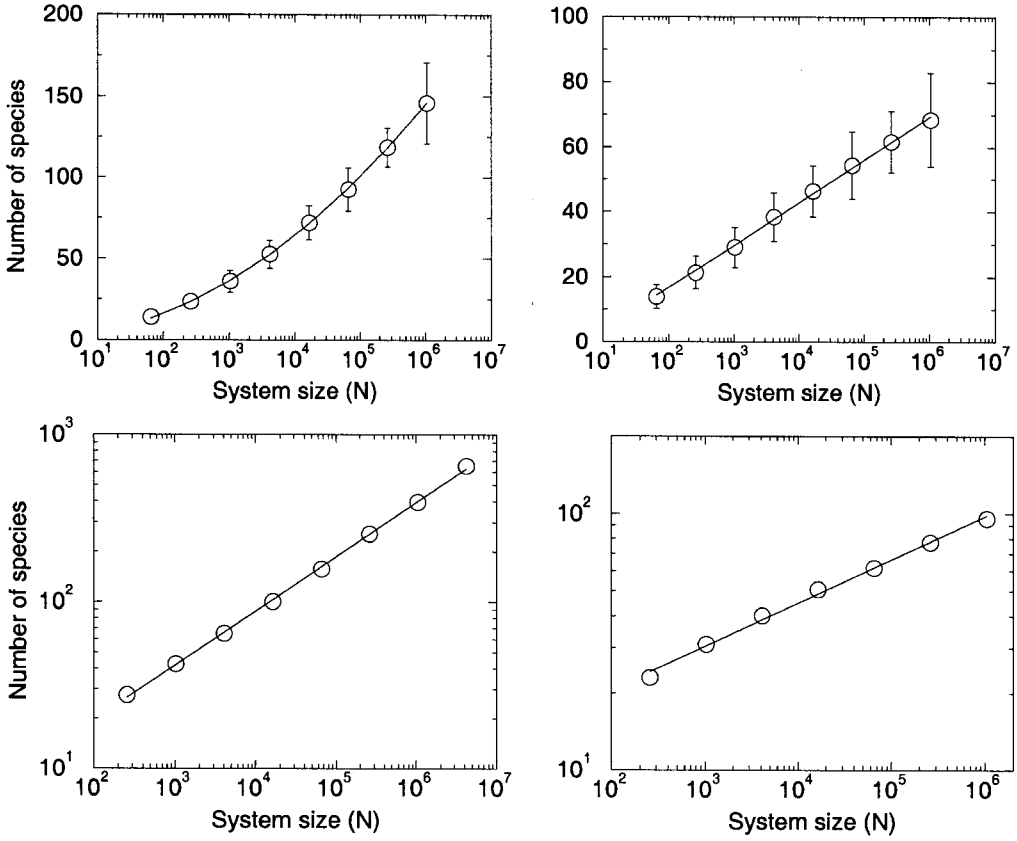

Figure 11: Scaling function $F(N, \theta, \sigma)$ in the neutral model (*top*) and in the trade-off model (*bottom*) under nearest-neighbor dispersal ($\sigma = 1$; *left*) and global dispersal (*right*). For all simulations, $\theta = 5$. All points are means of 40–400 simulations each; the brackets show standard deviations. For nearest-neighbor dispersal in the neutral models, equation (6) predicts $S = (\theta/2\pi\sigma^2)[\ln(N)]^2 = 0.796[\ln(N)]^2$, while the best fit is $S = 0.759[\ln(N)]^2$ (*line, top left*). For global dispersal, equation (3) predicts $S = \theta \ln(1 + N/\theta) = 5\ln(1 + N/5)$, while the best fit is for $S = 5.73\ln(1 + N/5.73)$ (*line, top right*). Both curves of the trade-off model exhibit power-law behavior with slope $z = 0.325(4)$ for the nearest-neighbor dispersal case (*bottom left*) and $z = 0.169(5)$ for the global-dispersal case (*bottom right*). Note that axes are log-linear in the top panels and log-log in the bottom ones.

Conclusions and Future Directions

Our results show that there are some differences in community patterns that reflect differences in the processes at work in model communities, most important of which is the scale of dispersal. However, most of the patterns commonly investigated by ecologists are surprisingly robust to the presence or absence of niche differences between species and even the presence or absence of conspecific density dependence. Future work should examine whether they are similarly robust to habitat heterogeneity and habitat specialization, which have been hypothesized to be primary factors determining the slopes of species-area relationships at intermediate scales (Shmida and Wilson 1985). In addition, we should look for other community-level patterns that are more sensitive to the underlying processes; cluster size distributions of species may be such a pattern (J. B. Plotkin, J. Chave, and P. S. Ashton, unpublished manuscript).

In this article, we restrict ourselves to drawing qualitative conclusions about the effects of dispersal limitation, life-history niche difference, and conspecific density dependence because the strengths of these processes in the model are not based directly on data. Yet the most central questions are surely the relative quantitative impacts of these and other factors on species richness itself—how much would species richness decline if not for niche differences or density dependence or dispersal limitation? For most systems, experimental answers to these questions are impractical, if not impossible (but see Pacala and Rees 1998). The parameterization of models such as these through field measurements of processes offers a more feasible approach, one that has already shown promise in

forests of the northeastern United States (Pacala et al. 1996).

Acknowledgments

We thank F. Guichard, R. Nathan, and J. Plotkin for constructive comments on the manuscript and D. DeAngelis, P. Grubb, and S. Hubbell for insightful reviews. We gratefully acknowledge the support of the Andrew W. Mellon Foundation, the David and Lucile Packard Foundation (grant 99-8307), the National Science Foundation (H.C.M.-L.), the Smithsonian Tropical Research Institute (H.C.M.-L.), and the Princeton Environmental Institute (H.C.M.-L.).

APPENDIX A

Description of the Algorithms Used and Tests of Alternative Algorithms

Algorithms

Let A be the total number of sites in the landscape ($A = L^2$), m_s be the mortality rate of species s, f_s be the fecundity of species s, $K(r)$ be a dispersal kernel giving the probability of dispersing to a particular site a distance r away, and θ be the speciation rate. Then the following algorithms describe what happens in one time step in each of the models.

Neutral Model (*Algorithm N*)

Repeat A *times*: Pick a site at random. If this site is occupied, let the occupant die without regard to its species. The dead individual is immediately replaced by an offspring of one of its neighbors, chosen with probability $K(r)$ (where r is the distance between the two sites). The function $K(r)$ is the same for all species.

Repeat θ *times*: Pick a site at random and replace its occupant (if any) with an individual of a new species.

In the version of the neutral model with empty space, a site vacated by the death of an individual is reoccupied by an offspring of one of its neighbors with a probability <1.

Competition-Survival Trade-off Model, Version 2 (*Algorithm S1*)

Repeat A *times*: Pick a site at random. If this site is occupied, kill the occupant with probability m_s.

Repeat A *times*: Pick a site at random. If this site is occupied, let the occupant reproduce. That is, choose a neighboring site with probability $K(r)$ (where r is the distance between the two sites) and disperse an offspring to that site. If the neighboring site is empty, then the offspring establishes there. If the neighboring site is occupied, then the individual of the species with the higher mortality rate (whether the resident or the offspring) wins the site.

Repeat θ *times*: Pick a site at random and replace its occupant (if any) with an individual of a new species. Choose the mortality rate m_s of the new species from a uniform distribution on [0, 1].

Competition-Survival Trade-off Model, Version 1 (*Algorithm S2*)

Repeat A *times*: Pick a site at random. If this site is occupied by an individual of species s, then kill the occupant (with probability $m_s/2$) or let it reproduce (with probability one-half) or do nothing (with probability $[1 - m_s]/2$). If this individual reproduces, then choose a neighboring site with probability $K(r)$ (where r is the distance between the two sites) and disperse an offspring to that site. If the neighboring site is empty, then the offspring establishes there. If the neighboring site is occupied, then the individual of the species with the higher mortality rate (whether the resident or the offspring) wins the site.

Repeat θ *times*: Pick a site at random and replace its occupant (if any) with an individual of a new species. Choose the mortality rate m_s of the new species from a uniform distribution on [0, 1].

Competition-Fecundity Trade-off Model (*Algorithm F*)

Repeat A *times*: Pick a site at random. If this site is occupied by an individual of species s, then kill the occupant (with probability $m_s/2$) or let it reproduce (with probability one-half) or do nothing (with probability $[1 - m_s]/2$). If this individual reproduces, then it produces an average of f_s offspring. For each offspring, a neighboring site is chosen with probability $K(r)$ (where r is the distance between the two sites), and the offspring is dispersed to this site. If the neighboring site is empty, then the offspring establishes there. If the neighboring site is occupied, then the individual of the species with the lower fecundity (whether the resident or the offspring) wins the site.

Repeat θ *times*: Pick a site at random and replace its occupant (if any) with an individual of a new species. Choose the fecundity f_s such that a number x is drawn from a uniform distribution on $[1/F_{\max}, 1]$. The integer f_s is then obtained by taking the integer value of $1/x + \zeta$, where ζ is a random number drawn from a uniform distribution on [0, 1].

Comparisons among Alternatives

To establish the robustness of our results to the details of our implementation, we compared various alternative algorithms. None of the variations that we tested led to changes in the qualitative patterns that we emphasize, al-

though most did cause small changes in the equilibrium number of species maintained in the system.

In the case of the neutral model (algorithm N), there are relatively few alternative implementations because of its very simplicity. The influence of including a death rate in the neutral model is discussed in "Species Richness." Hubbell (2001) explores the effects of different types of speciation on the neutral model and finds that speciation by random fission of existing populations greatly increases species richness. Dornic et al. (2001) have recently shown that the neutral model is the simplest example of a large class of models that exhibit the same emergent behavior, that is, the same coarsening properties.

The trade-off models admit more alternative implementations. We examined the effects of three types of variations on the competition-survival trade-off model. First, we compared the two algorithms for the competition-survival trade-off explained above (algorithms S1 and S2). The results presented in the body of the article were obtained using algorithm S1, which might be called a "seasonal" algorithm since all deaths in a time step occur together and precede all births. An alternative is to implement "aseasonal" dynamics, in which births and deaths are continually interspersed (algorithm S2). When dynamics were implemented in an aseasonal manner, such that births and deaths were interspersed, the number of species at equilibrium in any particular run increased. However, the shapes of all relationships examined remained the same (results not shown).

Second, we tested whether the trade-off-model results were robust to the manner in which mortality rates are assigned to new species. We ran additional simulations in which the mortality rates of new species were "mutations" on those of existing species in the system. In the usual implementation, new species are assigned mortality rates chosen at random between 0 and 1. Assigning new species mortality rates similar to those of existing ones also means that in the local-dispersal models, fewer new species have fundamentally unviable mortality rates—rates so high that they could not persist even if they were alone in the system. (For the nearest-neighbor case, mortality rates above approximately 0.62 are unviable.) If mutation rates of new species are chosen from a Gaussian distribution around those of an existing "parent" species, a "memory effect" is present in the model, and dynamic equilibrium is reached after a longer transient. The equilibrium patterns, however, remain much the same.

Third, we tested whether the results were robust to changes in the way in which individuals of new species are placed in the model landscape. For the main simulations, individuals are placed at random in the landscape. An alternative is to have randomly chosen new offspring become individuals of a new species with some probability. This means that individuals of new species show the same biases in where they appear as do offspring of existing species; this may, for instance, mean more new species in areas of high occupancy and fewer in areas of low occupancy. If all the sites are equally likely to have propagules land on them, then these two mechanisms are equivalent; this will be the case when there are no empty cells and/or when dispersal is global. For the trade-off model and local dispersal, however, these two formulations will not be equivalent. We thus performed additional runs in which new species were placed randomly among sites that would have received a dispersing offspring, rather than randomly among all sites. Both formulations produce equivalent results.

APPENDIX B

The Bramson-Cox-Durrett Theorem for the Scaling-Function Problem

We here present the main result proved in Bramson et al. (1998).

Theorem. Let $K_\sigma(r)$ be the distribution of step sizes of the random walk (i.e., $K_\sigma(r)$ is the dispersal kernel) with mean dispersal distance σ. Let $V_\sigma(t)$ be the number of distinct sites visited in t time steps by a random walk with step size distributed according to $K_\sigma(r)$ on a regular lattice of edge L in d dimensions. For large N, the number of species in the d-dimensional multitype voter model with $N = L^d$ individuals and a mutation rate of θ new individuals per time step, the total number of species in the system, $F(N, \theta, \sigma)$, is related to $V_\sigma(t)$ by

$$F(N, \theta, \sigma) \approx \theta \int_1^N \frac{1}{V_\sigma(t)}\, dt. \tag{B1}$$

Note that both $F(N, \theta, \sigma)$ and $V_\sigma(t)$ are random variables. The mean number of species, $\overline{F}(N, \theta, \sigma)$, is also related to the mean number of sites visited, $\overline{V}(t)$, by equation (B1). Further, the standard deviation of the number of species can be deduced from the fact that $\sigma_V(t) \ll \overline{V}(t)$:

$$\overline{F}(N, \theta, \sigma) \simeq \theta \int_1^N \frac{1}{\overline{V}_\sigma(t)}\, dt,$$

$$\sigma_F(N, \theta, \sigma) \simeq \theta \int_1^N \frac{\sigma_V(t)}{\overline{V}_\sigma(t)^2}\, dt. \tag{B2}$$

(The sign "≈" in eq. [B1] means the two converge in distribution, while the sign "≃" in eq. [B2] means they converge in probability.) The functions $\overline{V}(t)$ and $\sigma_V(t)$ are known for many dispersal kernels because they are

part of classical probability theory (see, e.g., Weiss 1994; Hughes 1995).

We can find the scaling function by finding the form of $V_\sigma(t)$. Under global dispersal, the random walk essentially performs very long jumps, visiting a new site each time step, and thus, $V(t) = t$. Making use of equation (B1), we find $\overline{F}(N, \theta, \sigma) \simeq \theta \int_1^N dt/t$, which integrates to give $\overline{F}(N, \theta, \sigma) \simeq \theta \ln (N)$. In the case of nearest-neighbor dispersal in a two-dimensional lattice, we make use of the result of Dvoretzky and Erdős (1951), $\overline{V}(t) = \pi t/\ln (t)$, which yields $\overline{F}(N, \theta, \sigma) \simeq (1/2\pi\sigma^2)\theta[\ln (N)]^2$. Further, we can use equation (B2) and the fact that $\sigma_V(t) = c\sigma^2 t/\ln (t)^2$ (Torney 1986) to find the variance:

$$\sigma_F(N, \theta, \sigma) \simeq \frac{c}{\sigma^2\pi^2}\theta \ln (N). \tag{B3}$$

Thus, the relative error decreases extremely slowly (as $1/\ln (N)$).

As the variance of the dispersal kernel approaches the size of the system ($\sigma \approx L$), the picture is quantitatively different. This is the case for the fat-tail dispersal kernel of equation (2) for some values of parameter p. For $p > 1$, the variance is finite, and equation (6) holds. For $0 < p < 1$, the variance is infinite, although the dispersal kernel remains defined. In this case,

$$\overline{V}(t) = \begin{cases} t, & \text{if } p < 1 \\ \dfrac{bt}{\ln [\ln (t)^2]}, & \text{if } p = 1 \end{cases}, \tag{B4}$$

where b depends on the parameters p and u of the fat-tail kernel of equation (2) (see Gillis and Weiss 1970). For $p < 1$, formula (3) holds, while in the borderline case $p = 1$, a more complex formula holds, which we do not reproduce here.

Literature Cited

Armstrong, R. A. 1989. Competition, seed predation, and species coexistence. Journal of Theoretical Biology 141: 191–195.

Arrhenius, O. 1921. Species and area. Journal of Ecology 9:95–99.

Ashton, P. S. 1969. Speciation among tropical forest trees: some deductions in the light of recent evidence. Biological Journal of the Linnean Society 1:155–196.

———. 1998. Niche specificity among tropical trees: a question of scales. Pages 491–514 *in* D. M. Newbery, H. H. T. Prins, and N. D. Brown, eds. Dynamics of tropical communities. Blackwell Science, Oxford.

Ashton, P. S., and P. Hall. 1992. Comparisons of structure among mixed dipterocarp forests of northwestern Borneo. Journal of Ecology 80:459–481.

Ben Avraham, D., M. A. Burschka, and C. R. Doering. 1990. Statics and dynamics of a diffusion-limited reaction: anomalous kinetics, nonequilibrium self-ordering, and a dynamic transition. Journal of Statistical Physics 60: 695–728.

Botkin, D. B., J. F. Janik, and J. R. Wallis. 1972. Some ecological consequences of a computer model of forest growth. Journal of Ecology 60:849–872.

Bramson, M., J. T. Cox, and R. Durrett. 1996. Spatial models for species area curves. Annals of Probability 24:1727–1751.

———. 1998. A spatial model for the abundance of species. Annals of Probability 26:658–709.

Buttel, L., R. Durrett, and S. Levin. In press. Competition and species packing in patchy environments. Theoretical Population Biology.

Caley, M. J., M. H. Carr, M. A. Hixon, T. P. Hughes, G. P. Jones, and B. A. Menge. 1996. Recruitment and the local dynamics of open marine populations. Annual Review of Ecology and Systematics 27:477–500.

Canham, C. D., A. C. Finzi, S. W. Pacala, and D. H. Burbank. 1994. Causes and consequences of resource heterogeneity in forests: interspecific variation in light transmission by canopy trees. Canadian Journal of Forest Research 24:337–349.

Caswell, H. 1976. Community structure: a neutral model analysis. Ecological Monographs 46:327–354.

Chave, J. 2001. Spatial patterns and persistence of woody species in ecological communities. American Naturalist 157:51–65.

Chesson, P. L., and R. R. Warner. 1981. Environmental variability promotes coexistence in lottery competitive systems. American Naturalist 117:923–943.

Clark, J. S., M. Silman, R. Kern, E. Macklin, and J. HilleRisLambers. 1999. Seed dispersal near and far: patterns across temperate and tropical forests. Ecology 80: 1475–1494.

Clifford, P., and A. Sudbury. 1973. A model for spatial conflict. Biometrika 60:581–588.

Coleman, B. D. 1981. On random placement and species-area relations. Mathematical Biosciences 54:191–225.

Condit, R., S. P. Hubbell, and R. B. Foster. 1992. Recruitment near conspecific adults and the maintenance of tree and shrub diversity in a Neotropical forest. American Naturalist 140:261–286.

Condit, R., S. P. Hubbell, J. V. LaFrankie, R. Sukumar, N. Manokaran, R. B. Foster, and P. S. Ashton. 1996. Species-area and species-individual relationships for tropical trees: a comparison of three 50-ha plots. Journal of Ecology 84:549–562.

Connell, J. H. 1971. On the roles of natural enemies in

preventing competitive exclusion in some marine animals and in rain forest trees. Pages 298–312 *in* P. J. den Boer and G. R. Gradwell, eds. Dynamics of populations. Proceedings of the Advanced Study Institute on "Dynamics of Numbers in Populations," Oosterbeek, Netherlands. Pudoc, Wageningen.

———. 1979. Tropical rain forests and coral reefs as open nonequilibrium systems. Pages 141–163 *in* R. M. Anderson, B. D. Turner, and L. R. Taylor, eds. Plant population ecology. Blackwell Scientific, Oxford.

Connor, E. F., and E. D. McCoy. 1979. The statistics and biology of the species-area relationship. American Naturalist 113:791–833.

Connor, E. F., and D. Simberloff. 1979. The assembly of species communities: chance or competition? Ecology 60:1132–1140.

Crawley, M. J. 1997. Plant Ecology. 2d ed. Blackwell Science, Oxford.

Dalling, J. W., S. P. Hubbell, and K. Silvera. 1998. Seed dispersal, seedling establishment and gap partitioning among tropical pioneer trees. Journal of Ecology 86: 674–689.

Dornic, I., H. Chaté, J. Chave, and H. Hinrichsen. 2001. Critical coarsening without surface tension: the universality class of the voter model. Physical Review Letters 87:045701.

Durrett, R. 1988. Lecture notes on particle systems and percolation. Wadsworth & Brooks/Cole Advanced Books & Software, Pacific Grove, Calif.

Durrett, R., and S. A. Levin. 1994. The importance of being discrete (and spatial). Theoretical Population Biology 46:361–394.

———. 1996. Spatial models for species area curves. Journal of Theoretical Biology 179:119–127.

———. 1998. Spatial aspects of interspecific competition. Theoretical Population Biology 53:30–43. Erratum 53: 284.

Dvoretzky, A., and P. Erdős. 1951. Some problems on random walk in space. Pages 353–367 *in* J. Neyman, ed. Proceedings of the Second Berkeley Symposium on Mathematical Statistics and Probability. University of California Press, Berkeley.

Ewens, W. J. 1972. The sampling theory of selectively neutral alleles. Theoretical Population Biology 3:87–112.

Fisher, R. A., A. S. Corbet, and C. B. Williams. 1943. The relation between the number of species and the number of individuals in a random sample of an animal population. Journal of Animal Ecology 12:42–58.

Gillis, J. E., and G. H. Weiss. 1970. Expected number of distinct sites visited by a random walk with an infinite variance. Journal of Mathematical Physics 11:1307–1312.

Greig-Smith, P. 1952. The use of random contiguous quadrats in the study of the structure of plant communities. Annals of Botany 16:293–316.

Grubb, P. 1977. The maintenance of species richness in plant communities: the importance of the regeneration niche. Biological Reviews 53:107–145.

Hammond, D. S., and V. K. Brown. 1998. Disturbance, phenology and life-history characteristics: factors influencing distance/density-dependent attack on tropical seeds and seedlings. Pages 51–78 *in* D. M. Newbery, H. H. T. Prins, and N. D. Brown, eds. Dynamics of tropical communities. Blackwell Science, Oxford.

Harms, K. E., S. J. Wright, O. Calderon, A. Hernandez, and E. A. Herre. 2000. Pervasive density-dependent recruitment enhances seedling diversity in a tropical forest. Nature 404:493–495.

Harper, J. L. 1977. Population biology of plants. Academic Press, London.

Hastings, A. 1980. Disturbance, coexistence, history, and competition for space. Theoretical Population Biology 18:363–373.

Holley, R., and T. M. Liggett. 1975. Ergodic theorems for weakly interacting systems and the voter model. Annals of Probability 3:643–663.

Holt, R. D. 1992. A neglected facet of island biogeography: the role of internal spatial dynamics in area effects. Theoretical Population Biology 41:354–371.

Horn, H. S., and R. H. MacArthur. 1972. Competition among fugitive species in a harlequin environment. Ecology 53:749–752.

Hubbell, S. P. 1979. Tree dispersion, abundance and diversity in a dry tropical forest. Science (Washington, D.C.) 203:1299–1309.

———. 1995. Toward a theory of biodiversity and biogeography on continuous landscapes. Pages 171–199 *in* G. Carmichael, G. Folk, and J. Schnoor, eds. Preparing for global change: a midwestern perspective. SPB Academic, Amsterdam.

———. 1997. A unified theory of biogeography and relative species abundance and its application to tropical rain forests and coral reefs. Coral Reefs 16:S9–S21.

———. 2001. A unified neutral theory of biogeography. Princeton University Press, Princeton, N.J.

Hughes, B. D. 1995. Random walks and random environments. Vol. 1. Random walks. Clarendon, Oxford.

Hutchinson, G. E. 1959. Homage to Santa Rosalia, or why are there so many kinds of animals? American Naturalist 93:145–159.

Janzen, D. H. 1970. Herbivores and the number of tree species in tropical forests. American Naturalist 104: 501–528.

Kinzig, A. P., S. A. Levin, J. Dushoff, and S. Pacala. 1999. Limiting similarity, species packing, and system stability

for hierarchical competition-colonization models. American Naturalist 153:371–383.

Kot, M., M. A. Lewis, and P. van der Driessche. 1996. Dispersal data and the spread of invading organisms. Ecology 77:2027–2042.

Levin, S. A. 1976. Population dynamic models in heterogeneous environments. Annual Review of Ecology and Systematics 7:287–310.

Levin, S. A., and H. C. Muller-Landau. 2000. The evolution of dispersal and seed-size in plant colonies. Evolutionary Ecology Research 2:409–435.

Levins, R. 1970. Extinction. Pages 75–108 *in* M. Gerstenhaber, ed. Some mathematical questions in biology. American Mathematical Society, Providence, R.I.

Levins, R., and D. Culver. 1971. Regional coexistence of species and competition between rare species. Proceedings of the National Academy of Sciences of the USA 68:1246–1248.

MacArthur, R. H. 1960. On the relative abundance of species. American Naturalist 45:25–36.

MacArthur, R. H., and E. O. Wilson. 1967. The theory of island biogeography. Princeton University Press, Princeton, N.J.

May, R. M. 1975. Patterns of species abundance and diversity. Pages 81–120 *in* M. L. Cody and J. M. Diamond, eds. Ecology and evolution of communities. Belknap, Cambridge, Mass.

May, R. M., and M. A. Nowak. 1994. Superinfection, metapopulation dynamics, and the evolution of diversity. Journal of Theoretical Biology 170:95–114.

McGuinness, K. A. 1984. Equations and explanations in the study of species-area curves. Biological Reviews 59: 423–440.

Molofsky, J., R. Durrett, J. Dushoff, D. Griffeath, and S. Levin. 1999. Local frequency dependence and global coexistence. Theoretical Population Biology 55:270–282.

Nathan, R., and H. C. Muller-Landau. 2000. Spatial patterns of seed dispersal, their determinants and consequences for recruitment. Trends in Ecology & Evolution 15:259–302.

Newbery, D. M., and J. Proctor. 1984. Ecological studies in four contrasting lowland rain forests in Gunung Mulu National Park, Sarawak. IV. Associations between tree distribution and soil factors. Journal of Ecology 72: 475–493.

Nowak, M. A., and R. M. May. 1994. Superinfection and the evolution of parasite virulence. Proceedings of the Royal Society of London B, Biological Sciences 55: 81–89.

Ouborg, N. J., Y. Piquot, and J. M. van Groenendael. 1999. Population genetics, molecular markers and the study of dispersal in plants. Journal of Ecology 87:551–568.

Pacala, S. W., and S. A. Levin. 1997. Biologically generated spatial pattern and the coexistence of competing species. Pages 204–232 *in* D. Tilman and P. Kareiva, eds. The role of space in population dynamics and interspecific interactions. Princeton University Press, Princeton, N.J.

Pacala, S. W., and M. Rees. 1998. Models suggesting field experiments to test two hypotheses explaining successional diversity. American Naturalist 152:729–737.

Pacala, S. W., and D. Tilman. 1993. Limiting similarity in mechanistic and spatial models of plant competition in heterogeneous environments. American Naturalist 143: 222–257.

Pacala, S. W., C. D. Canham, J. Saponara, J. Silander, R. Kobe, and E. Ribbens. 1996. Forest models defined by field measurements. II. Estimation, error analysis and dynamics. Ecological Monographs 66:1–43.

Packer, A., and K. Clay. 2000. Soil pathogens and spatial patterns of seedling mortality in a temperate tree. Nature 404:278–281.

Paine, R. T. 1966. Food web complexity and species diversity. American Naturalist 100:65–75.

Pitman, N. C. A., J. Terborgh, M. R. Silman, and P. Nuñez. 1999. Tree species distributions in an upper Amazonian forest. Ecology 80:2651–2661.

Plotkin, J. B., M. D. Potts, D. W. Yu, S. Bunyavejchewin, R. Condit, R. Foster, S. Hubbell, et al. 2000*a*. Predicting species diversity in tropical forests. Proceedings of the National Academy of Sciences of the USA 97: 10850–10854.

Plotkin, J. B., M. D. Potts, N. Leslie, N. Manokaran, J. LaFrankie, and P. S. Ashton. 2000*b*. Species-area curves, spatial aggregation, and habitat specialization in tropical forests. Journal of Theoretical Biology 207:81–99.

Preston, F. W. 1962. The canonical distribution of commonness and rarity. Ecology 43:185–215, 410–432.

Rabinowitz, D. 1981. Seven forms of rarity. Pages 205–217 *in* H. Synge, ed. The biological aspects of rare plant conservation. Wiley, New York.

Rosenzweig, M. L. 1995. Species diversity in space and time. Cambridge University Press, Cambridge.

Salo, J., R. Kalliola, I. Häkkinen, Y. Mäkinen, P. Niemelä, M. Puhakka, and P. D. Coley. 1986. River dynamics and the diversity of Amazon lowland forest. Nature 322: 254–258.

Shmida, A., and M. V. Wilson. 1985. Biological determinants of species diversity. Journal of Biogeography 12: 1–20.

Shugart, H. H. 1984. A theory of forest dynamics. Springer, New York.

Simberloff, D. S. 1976. Species turnover and equilibrium island biogeography. Science (Washington, D.C.) 194: 572–578.

Sugihara, G. 1980. Minimal community structure: an ex-

planation of species abundance patterns. American Naturalist 116:770–787.

Terborgh, J., and J. Andresen. 1998. The composition of Amazonian forests: patterns at local and regional scales. Journal of Tropical Ecology 14:645–664.

Terborgh, J., R. B. Foster, and P. Nuñez. 1996. Tropical tree communities: a test of the nonequilibrium hypothesis. Ecology 77:561–567.

Thorson, G. 1950. Reproductive and larval ecology of marine bottom invertebrates. Biological Reviews 25:1–45.

Tilman, D. 1994. Competition and biodiversity in spatially structured habitats. Ecology 75:2–16.

Tilman, D., and S. W. Pacala. 1993. The maintenance of species richness in plant communities. Pages 13–24 *in* R. E. Ricklefs and D. Schluter, eds. Species diversity in ecological communities: historic and geographical perspectives. University of Chicago Press, Chicago.

Torney, D. C. 1986. Variance of the range of a random walk. Journal of Statistical Physics 44:49–66.

Watterson, G. A. 1974. The sampling theory of selectivity neutral alleles. Advances in Applied Probability 6: 463–488.

Weiss, G. H. 1994. Aspects and applications of the random walk (random materials and processes). North-Holland Publishing, Amsterdam.

Whittaker, R. H. 1972. Evolution and measurement of species diversity. Taxon 21:213–251.

Willson, M. F. 1993. Dispersal mode, seed shadows, and colonization patterns. Vegetatio 107/108:261–280.

Wright, S. J. 1981. Intra-archipelago vertebrate distribution: the slope of the species-area relation. American Naturalist 118:726–748.

Yu, D. W., J. W. Terborgh, and M. D. Potts. 1998. Can high tree species richness be explained by Hubbell's null model? Ecology Letters 1:193–199.

Zhang, D. Y., and K. Lin. 1997. The effects of competitive asymmetry on the rate of competitive displacement: how robust is Hubbell's community drift model? Journal of Theoretical Biology 188:361–367.

Associate Editor: Donald L. DeAngelis